

# On the inspiral of massive black holes in gas-rich galaxy mergers

M. Colpi<sup>\*</sup>, S. Callegari<sup>†</sup>, M. Dotti<sup>\*\*</sup>, S. Kazantzidis<sup>‡</sup> and L. Mayer<sup>†,§</sup>

<sup>\*</sup>*Dipartimento di Fisica G. Occhialini, Università degli Studi di Milano Bicocca, Piazza della Scienza 3, 20126 Milano, Italy*

<sup>†</sup>*Institute for Theoretical Physics, University of Zürich, Winterthurerstrasse 190, CH-8057 Zürich, Switzerland*

<sup>\*\*</sup>*Dipartimento di Fisica e Matematica, Università dell'Insubria, Via Valleggio 11, 22100 Como, Italy*

<sup>‡</sup>*Kavli Institute for Particle Astrophysics and Cosmology, Department of Physics, Stanford University, MS 29, Stanford, California 94309, USA*

<sup>§</sup>*Institute of Astronomy, ETH Zürich-Hönggerberg, CH-8093 Zürich, Switzerland*

**Abstract.** We present a study on the dynamics of massive black holes (BHs) in galaxy mergers, obtained from a series of high-resolution N-Body/SPH simulations. We show that the presence of a gaseous component is essential for the rapid formation of an eccentric (Keplerian) BH binary. The binary resides at the center of a massive ( $\sim 10^9 M_\odot$ ) turbulent nuclear disc resulting from the collision of the two gaseous discs present in the parent galaxies. Using physically and/or numerically motivated recipes, we follow the accretion history of the BHs during the merger. We find that the mass of the BHs increases as large central inflows of gas occur inside each galaxy, and that the mass ratio  $q_{\text{BH}}$  varies with time indicating that the memory of its initial value may be lost. Given the uncertainties in the accretion recipes and the encountered strong degeneracy between numerical resolution and physical assumptions, we suggest here three possible paths followed by the galaxies and the BHs during a merger in order to fulfill the  $M_{\text{BH}}$  versus  $\sigma$  relation : *Adjustment*, *Symbiosis*, and *BH Dominance*. In an extremely high resolution run, we resolved the turbulent gas pattern down to parsec scales, and found that BH feedback is expected to be effective near the end of the merger. We then trace the BH binary orbit down to a scale of 0.1 pc modeling the nuclear disc, resulting from the galaxy collision, as an equilibrium Mestel disc composed either of gas, gas and stars, or just stars. Under the action of dynamical friction against the rotating gaseous and/or stellar background the orbit circularizes. When this occurs, each BH is endowed with its own small-size ( $\ll 0.01$  pc) accretion disc comprising a few percent of the BH mass. Double AGN activity is expected to occur on an estimated timescale of  $\lesssim 10$  Myrs, comparable to the inspiral time. The double nuclear point-like sources that may appear have typical separations of  $\lesssim 10$  pc, and are likely to be embedded in the still ongoing starburst.

**Keywords:** Black hole physics – hydrodynamics – galaxies: starburst – galaxies: evolution – galaxies: nuclei

**PACS:** PACS Number 98.54

## I. GALAXY COLLISIONS WITH MASSIVE BLACK HOLES

In this section we explore the dynamics of supermassive black holes (BHs) in gas-rich galaxy mergers resulting from high-resolution N-Body/SPH simulations carried out with Gasoline [1]. The initial galaxy models comprise a dark matter halo, a disc with 10% of its total mass in the form of gas, a bulge and a BH treated as softened particle; the reference galaxy reproduces the Milky Way with its central black hole ( $M_{\text{BH}} =$

$3 \times 10^6 M_\odot$ ). Encounters with mass ratio  $q = M_2/M_1$  equal to 1 and 1/4 are explored, the smaller galaxy ( $M_2$ ) being a rescaled replica of the Milky Way like reference model; the BH mass ratio  $q_{\text{BH}}$  is the same as  $q$ , according to the Magorrian relation [2]. Atomic cooling down to a floor temperature of 20,000 K, and star formation are accounted for in the simulations (see [3] for details).

First, the merger and BH inspiral is followed from the large scale  $\sim 100$  kpc down to  $\sim 200$  pc which is our force resolution limit. In a second run, we apply the technique of particle splitting to follow the gas thermodynamics and the massive BH inspiral down to a force resolution of 4 pc (see [4]).

- **BH DYNAMICS down to 200 pc:** In encounters between gas-rich galaxies with  $q = 1$  (“major” mergers) the BHs, dragged together with their more massive bulges, lose orbital angular momentum under the action of dynamical friction. After  $\sim 5$  Gyr, the BHs form a close pair. They orbit inside a massive ( $\sim 10^9 M_\odot$ ) self-gravitating nuclear disc formed at the end of the merger [5]. In gas-free encounters with  $q = 1$ , the BHs sink at the center of the remnant forming again a close pair with separations solely limited by the force resolution.

By contrast, in encounters with  $q = 1/4$  (“minor” mergers) the final separation of the BHs depends sensitively on how the central structure of the merging galaxies is affected by gaseous dissipation. When absent (i.e., in dry mergers), mass loss induced by tidal forces disrupt the secondary, lighter galaxy, leaving the less massive BH wandering at a distance of several kpc away from the center of the remnant. In contrast, gas cooling facilitates the pairing of the two BHs (down to 200 pc) by increasing the resilience of the secondary galaxy to tidal disruption.

- **BH DYNAMICS down to 4 pc:** In the case of a major ( $q = 1$ ) coplanar merger, we continued the simulation using the technique of particle splitting to explore the BH dynamics on a scale of few parsecs [4]. We find that *the inspiral of the two BHs proceeds down to a distance at which a close Keplerian binary forms*. Their sinking is controlled fully by the gaseous component under the typical conditions of a starburst. The BHs are found to move on a mildly eccentric orbit inside a  $\sim 10^9 M_\odot$  rotationally supported, turbulent nuclear disc of size  $\sim 40$  pc [6].

- **ACCRETION and BH GROWTH:** The simulations covered a dynamical range of 5 orders of magnitude (in total) from the scale of 100 kpc down to 4 pc, and only in the refined run the force limit was becoming comparable to the gravitational sphere of influence of the BHs: for this reason, we could not probe the flow pattern around each individual BH along the course of their evolution with enough accuracy to assess the magnitude of the accretion rate  $\dot{M}_{\text{BH}}$ . We thus applied different recipes for  $\dot{M}_{\text{BH}}$  in order to extract information about the “possible” mass growth from the N-body/SPH run of a  $q = 1/4$  merger with gas cooling and star formation.

We first considered a standard Bondi Eddington limited accretion recipe for  $\dot{M}_{\text{BH}}$ . The density of the gas around each massive BH is computed within a spherical radius twice our force softening (i.e., 200 pc in the less resolved simulations, and 4 pc in the high resolution run). As reference speed for the gas in the Bondi formula we considered either the thermal sound speed in the vicinity of the BHs ( $\sim 15 \text{ km s}^{-1}$ ), or we hypothesized a turbulent velocity for the gas  $\sim 60 \text{ km s}^{-1}$ : such turbulent motions are not resolved in the low resolution simulations and are thus simply considered as they are observed in

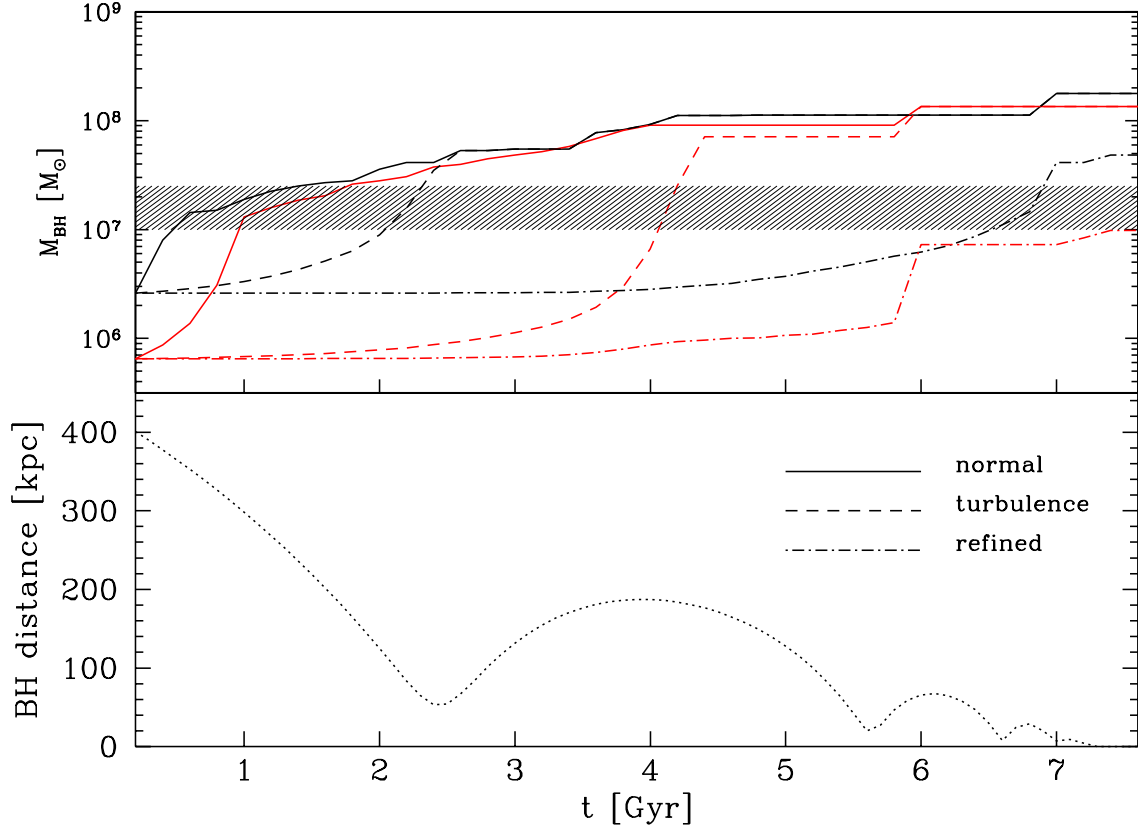


**FIGURE 1.** In the upper panel, different histories for the mass growth of the primary and secondary BHs are shown in black and red, respectively, for an encounter with  $q_{\text{BH}} = 1/4$ . Solid lines refer to standard Bondi-Hoyle accretion, dashed lines show results following from the assumption of turbulent motions, and dot-dashed lines trace the accretion history obtained extrapolating data from the refined simulation. In the lower panel, the relative distance of the two BHs during the merger is plotted.

circumnuclear discs of merger remnants [7]. Instead, in the high resolution simulation we measured turbulent velocities of such magnitude for the gas particles in the nuclear disc. They arise as a result of the final supersonic collision between the two gaseous galaxy cores and persist because of the inefficient dissipation implied by the effective equation of state of the nuclear gas subject to the starburst.

Figure 1 shows in its lower panel the BH relative distance as a function of time, and, in its upper panel, the corresponding mass growth of the BH. The black (red) solid line describes the mass of the primary (secondary) BH as a function of time, obtained from the low-resolution simulations using the thermal sound speed in the Bondi formula. Both BH masses grow initially not because of gas inflows stemming from the merger process, but simply because gas can be accreted inside a minimum volume fixed by the numerical resolution (200 pc). This volume is too large to allow for a realistic estimate of the gaseous mass effectively available (as seen in similar numerical experiments, even for isolated galaxies; see e.g. [8]). Further accretion episodes occur at every pericentric

passage. The long-dashed lines refer instead to accretion obtained by considering, for the same simulation, a typical turbulent sound speed. We see that mass growth occurs only after the tidal disturbances, excited during the merger, drive gas inflows towards the central regions of the interacting galaxies. In both cases the BHs become with time equally massive, and the memory of the initial ratio  $q_{\text{BH}}$  is lost. This is due to the relative importance of tides, that perturb more strongly the lighter galaxy.

At the end of the simulation, we extracted the value of the line-of-sight stellar velocity dispersion of the merger remnant inside  $1/8$  of the effective radius (obtained by fitting the stellar mass profile with a Sersic law [9] and averaging the result over different viewing angles). We then inferred the mass that the final relic BH would have in order to lie on the  $M_{\text{BH}}$  versus  $\sigma$  relation (shown as the shaded area in Figure 1). The two BH histories discussed above imply masses that are in excess of the expected value by an order of magnitude, even well before the merger is completed. These histories imply that the BHs may self-regulate their mass through AGN feedback on the surroundings “during the course of the merger”, sliding along the  $M_{\text{BH}}$  versus  $\sigma$  relation.

The limitations related to the force resolution appear clear when considering the third history (dot-dashed lines of Figure 1). In this last case, we extracted information about the density profile and the effective sound speed of the gas at a much closer distance (comparable to the BH gravitational sphere of influence) by rescaling results from a refined high resolution simulation of equal mass galaxies. These curves suggest that the BHs do not undergo any major growth during the first two orbits, and only when the galaxies merge the BH masses grow by more than an order of magnitude. The BH mass ratio varies with time but does not seem to increase toward unity. The primary BH is approaching and exceeding “from below” the  $M_{\text{BH}}$  versus  $\sigma$  expectation value, but in this case the final discrepancy is consistent with the scatter of the relation. The last episode of rapid mass growth may become self-regulated once feedback is included.

Given all these uncertainties on the BH mass growth, we can depict three possible (speculative) paths in the  $M_{\text{BH}}$  versus  $\sigma$  relation. Figure 2 shows these possibilities: (1) *Adjustment*: Adjustment occurs if the mass growth time  $\tau_{\text{growth}}$  of the individual BHs is long compared to the timescale of the merger  $\tau_{\text{merger}}$  (either because of turbulence or excess of angular momentum content in the gas near the massive BHs). The AGN phase would occur when the BHs are already in place at the center of the remnant galaxy, and self-regulation would result from balance between (thermal and/or mechanical) energy injection and gravitational energy of the surrounding gas. This can happen either before or after the final coalescence of the BH binary. In the first case, i.e., before coalescence, a double nuclear pointlike source could be detected in a star-bursting environment at separations closer than  $\simeq 10$  pc. (2) *Symbiosis*: In this case, both accretion and the buildup of the final galaxy occur almost synchronously ( $\tau_{\text{growth}} \sim \tau_{\text{merger}}$ ) with step-like episodes of AGN activity and starburst, leading to a “sliding” of  $M_{\text{BH}}$  and  $\sigma$  along the observed relation. In this case we may observe single or double AGN activity. If double, this would occur at separations from several kpc down to subparsec scales. (3) *BH Dominance*: BH growth is triggered by tidal torques during the early phase of the merger ( $\tau_{\text{growth}} < \tau_{\text{merger}}$ ), resulting in a mass exceeding the relation at intermediate stages; in this case the assembly of the galaxy would be dictated by the BH (BHs) that may regulate through its (their) luminosity the last starburst and the shape of the final potential well determining the  $\sigma$  of the remnant, though it is unclear how this could

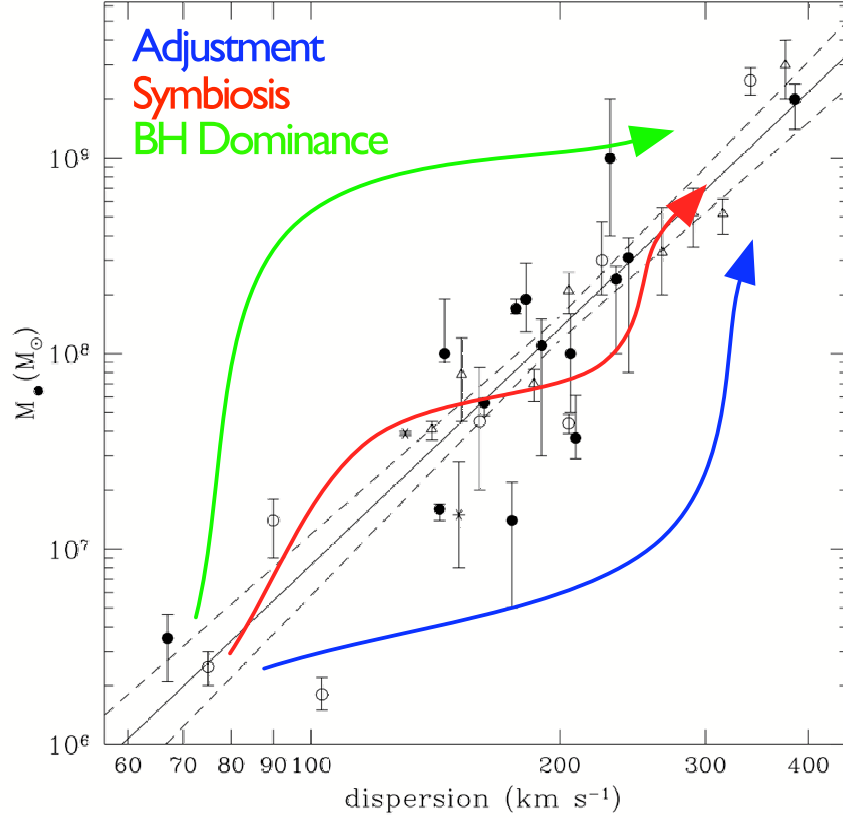


**FIGURE 2.** The three possible paths followed by galaxies and BHs during a merger in the BH mass versus stellar dispersion diagram from Tremaine et al. 2002 [17]. The green arrow shows the trend for the *BH Dominance* scenario, the red one refers to the *Symbiosis* scenario, the blue to *Adjustment*.

produce the higher velocity dispersion needed to satisfy the relation. In this scenario, luminous double AGN activity would be observed well before the two galaxies lose their identity, on very large scales.

Most theoretical efforts have been focused on the first scenario [10], [11] (see also [12]), and observations seem to find a low fraction of widely separated, interacting galaxies hosting nuclear activity, thus disfavoring – albeit with some uncertainties – BH dominance as a general trend. On the other hand, numerical experiments on the scale of mergers with force resolution in the commonly employed range (at least an order of magnitude larger than the sphere of influence of a BH) indicate the third case as possible, and avoid/tune excessive BH mass growth by invoking a certain amount of local AGN feedback acting on the surrounding gas [8]. However, assessing with enough confidence which one of the three paths is actually followed would require convergence of results when going to higher resolution. Instead, the striking differences in the BH mass accretions shown in Figure 1 suggest that there is a strong degeneracy between numerical resolution and physical assumptions. In the absence of any feedback from the BH itself, higher numerical resolution produces the same delay in the growth of BHs

as unresolved turbulence. The high resolution simulations indicate that most of the BH growth occurs after the merger, which favors the "adjustment" scenario.

## II. BLACK HOLE DYNAMICS IN ROTATIONALLY SUPPORTED NUCLEAR DISCS

The last, independent series of simulations (carried out with Gadget; see [13]) trace the dynamics of a BH pair (with  $q_{\text{BH}} = 1, 1/4, 1/10$ ) orbiting inside a self-gravitating, rotationally supported disc (of  $10^8 M_\odot$ ) composed either of gas, gas and stars, or just stars [14],[15]. A primary BH (of mass  $4 \times 10^6 M_\odot$ ) is placed at the center of the disc, while a secondary is set on an eccentric orbit, according to the outcome of the large-scale simulation (see [4] and Part I). The disc has a radial Mestel profile, and a Toomre parameter  $> 3$  everywhere, to ensure stability.

Figure 3 shows the BH relative separation and orbital eccentricity as a function of time for  $q_{\text{BH}} = 1/4$  and a star-to-total mass ratio  $f_*$  in the disc of 0,  $1/3$ ,  $2/3$ , and 1, respectively. We find that dynamical friction against the gaseous and/or stellar background is responsible for the inspiral of the BH along the full orbit, and that the response of the background is insensitive to  $f_*$ , as the orbital motion of the secondary BH is highly supersonic [16].

All co-rotating, initially eccentric orbits circularize, as angular momentum loss by friction is less efficient than energy loss. Figure 4 shows the density perturbation excited by the secondary BH in the gas (left panels) and stellar (right panels) components at two different times, corresponding to the first passage at pericenter (upper panel), and apocenter (lower panel). The green curve shows the counterclockwise corotating orbit of the BH. Near pericenter, the BH has a speed larger than the local rotational velocity, so that dynamical friction causes a reduction of the velocity of the BH: the density wake lags behind the BH trail. On the contrary, near apocenter, the BH speed is lower than the disc rotational velocity, and, in this case, the force increases the orbital angular momentum since the wake is dragged in front of the BH trail. The net effect is a severe reduction of the eccentricity.

In the purely gaseous run with  $q_{\text{BH}} = 1$ , we spatially resolve, on sub-parsec scales, the gravitational sphere of influence of each BH (of the order of  $\simeq 6$  pc) to detail the mass profile of bound gas particles. We define as strongly (weakly) bound gas particles SBPs (WBPs) those found inside the sphere of influence with total energy per unit mass  $E = 0.5\Omega$  ( $E \sim 0$ ), where  $\Omega$  is the gravitational potential of each BH. We find that the mass collected by each BH is  $M_{\text{SBP}} \approx 0.02 M_{\text{BH}} \approx 8 \times 10^4 M_\odot$ , and  $M_{\text{WBP}} \approx 0.85 M_{\text{BH}} \approx 3.4 \times 10^6 M_\odot$ , respectively. These masses are of the same order for both the primary and secondary BHs, and remain constant in time as long as the BH separation is  $\gtrsim 1$  pc. At shorter relative distances the WBPs experience the tidal field of the binary so that they are no longer bound to the individual BH. At the end of the simulation  $M_{\text{WBP}}$  is smaller, as shown in Figure 5. At the same time the mass  $M_{\text{SBP}}$  associated to the primary (secondary) BH increases by a factor  $\approx 4$  ( $\approx 2.5$ ). Bound particles have a net angular momentum with respect to each BH, and form an ellipsoidal configuration which is pressure supported. The typical half-mass radii are similar for the two BHs:  $\simeq 3$  pc and  $\simeq 0.2$  pc for the WBPs and SBPs, respectively.

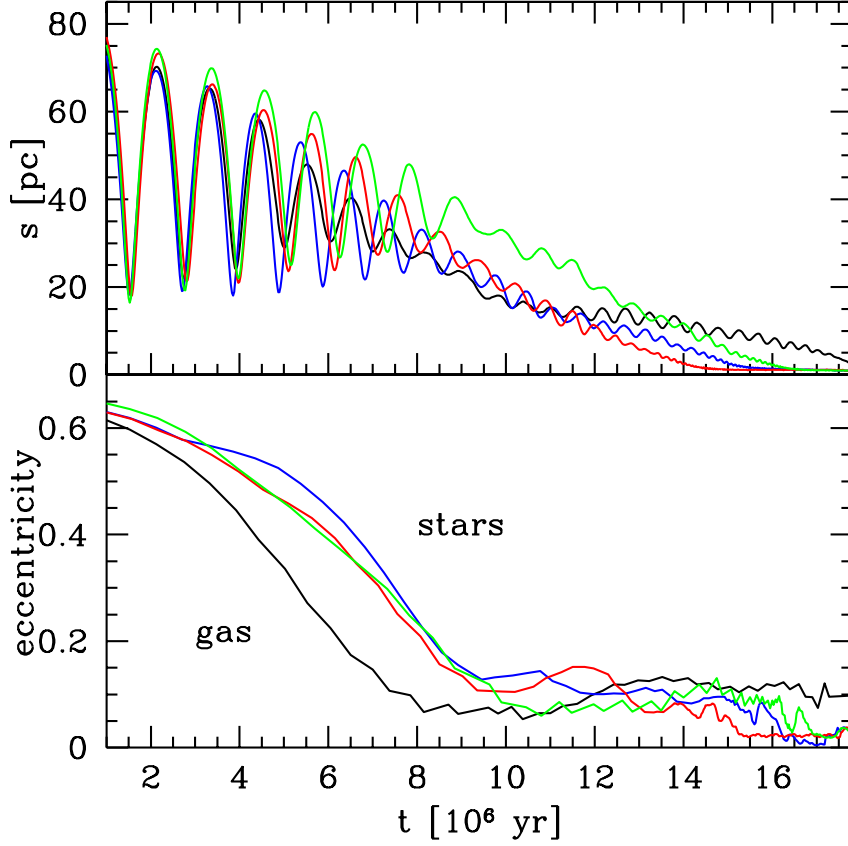


**FIGURE 3.** BH mass ratio 1/4. Upper panel: separations  $s$  (pc) between the BHs as a function of time. Lower panel: eccentricity of the BH binary as a function of time. Black, blue, red and green lines refer to stellar to total disc mass ratio  $f_*$  of 0, 1/3, 2/3 and 1. The two BHs form a binary for separations  $s < 5$  pc.

The disc gas density can be as high as  $10^7$  atoms  $\text{cm}^{-3}$ . It is then conceivable that, at these high densities, dissipative processes can be important, possibly reducing the gas internal (turbulent and thermal) energy well below the values adopted in our simulations. If dissipative processes reduce efficiently the gaseous internal energy, we expect that the bound gas will form a cool disc with Keplerian angular momentum comparable to what we found in our split simulation. We obtain for both the primary and the secondary BH a disc radius  $R_{\text{BH,disc}} \lesssim 0.01 \text{ pc}$  for the SBPs, a scale more than an order of magnitude below our best resolution limit. Our simplified treatment allows us to estimate a lower limit to the accretion timescale, assuming Eddington limited accretion:

$$t_{\text{acc}} = \frac{\epsilon}{1 - \epsilon} \tau_{\text{Edd}} \ln \left( 1 + \frac{M_{\text{acc}}}{M_{\text{BH},0}} \right), \quad (1)$$

where  $\epsilon$  is the radiative efficiency,  $\tau_{\text{Edd}}$  is the Eddington time,  $M_{\text{BH},0}$  is the initial mass of a BH, and  $M_{\text{acc}}$  is the mass of the accreted gas. Assuming  $\epsilon = 0.1$ , accretion can last at least 27 Myrs, and  $\lesssim 1$  Myrs, if the BHs accrete all the WBPs, and SWPs, respectively.

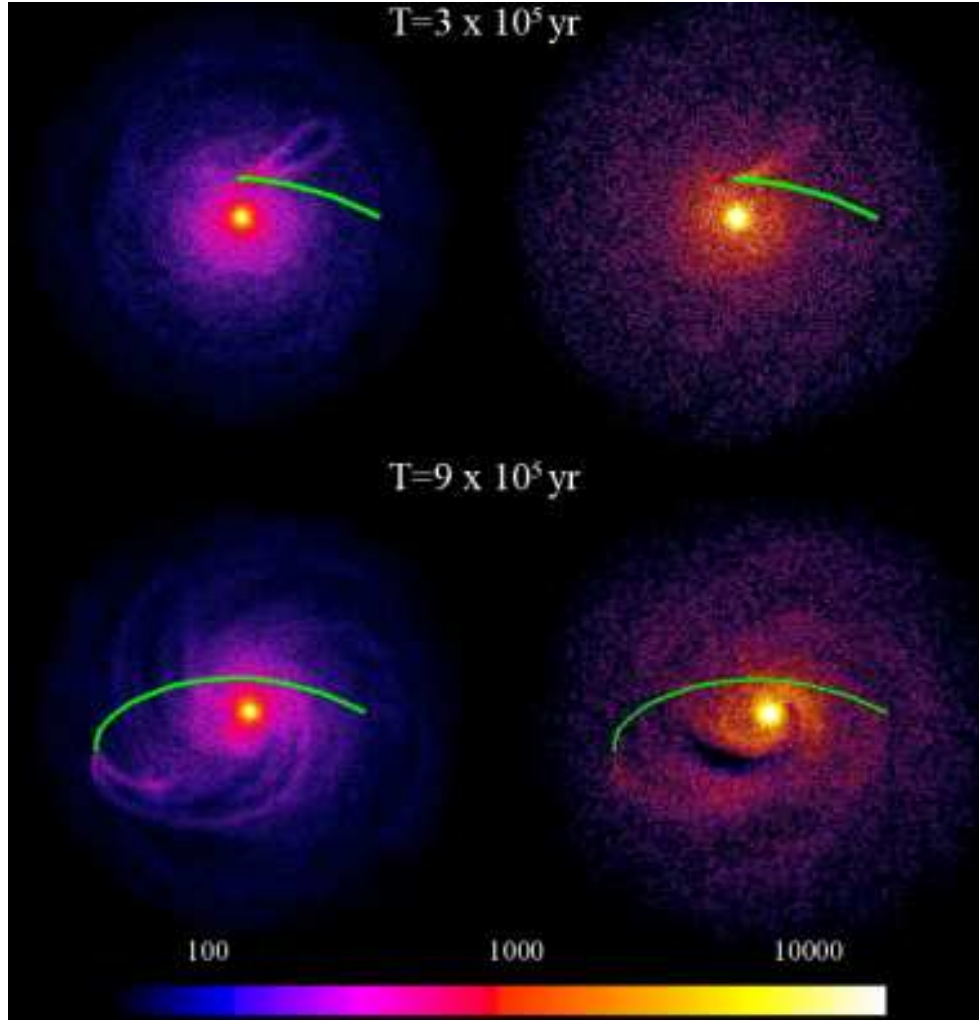


**FIGURE 4.** Snapshot from a simulation with both gaseous ( $2/3$  of the total disc mass) and stellar ( $1/3$ ) disc components seen face-on. The color coding indicates the  $z$ -averaged gas density (left panel) and star density (right panel) in logarithmic scale (units  $M_{\odot}/\text{pc}^3$ ). The green lines trace the secondary BH counterclockwise prograde orbit. The primary BH is present in the center of the disc. Each box size is 200 pc.

In summary, we have found that during the orbital inspiral, the gravitational attraction of each BH on surrounding gas particles is such that a gaseous mass comparable to the BH mass is present inside the BH sphere of influence and that 2% of this mass binds strongly to each single BH. The distribution of the most bound gas particles suggest that an active Eddington-limited accretion phase may set in, for a time  $\lesssim 1$  Myr around both BHs, with luminosities  $\sim 10^{44} \text{ erg s}^{-1}$ . The active phase could last for a longer time ( $\gtrsim 10$  Myr), comparable to the inspiral timescale, if all the bound mass is accreted. This highlights the possibility of revealing double AGN activity, on spatial scales  $\lesssim 10$  pc, embedded in a starburst. The small extension of the accretion disc around each BH could preserve the gas against tidal perturbation from the companion BH, and stripping until



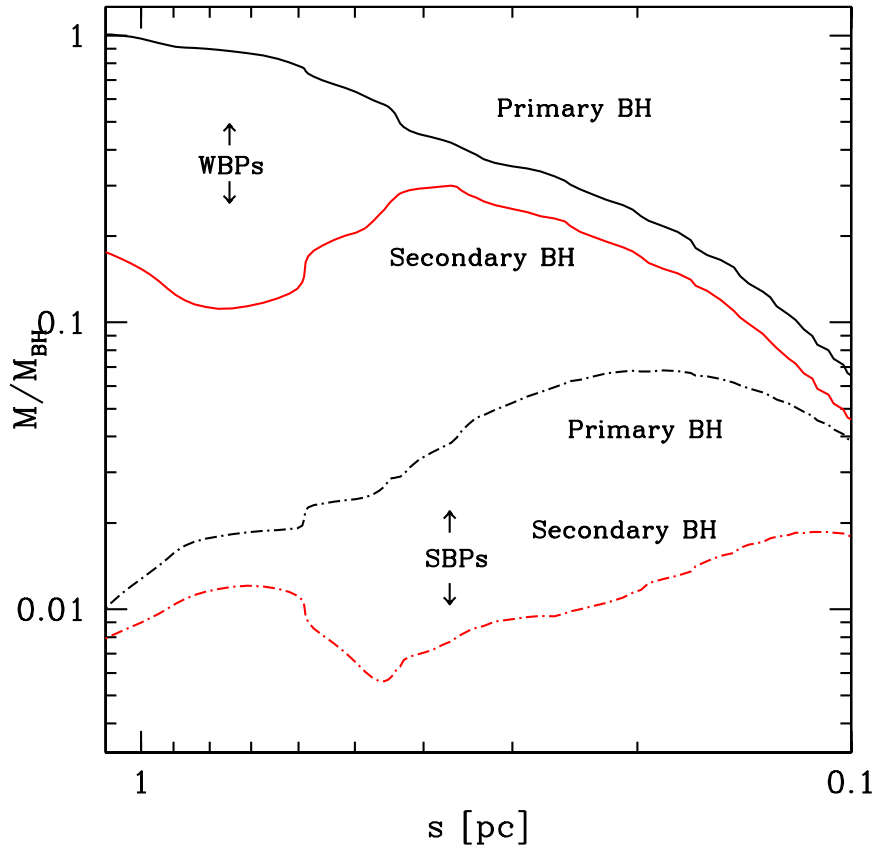


**FIGURE 5.** Masses of bound gas particles as a function of binary separation  $s$  in the final stages of the higher resolution simulation (between  $\approx 6$  and  $\approx 8.5$  Myrs after the onset of the simulation; see Fig. 3). Black lines refer to gas particles bound to the BH initially at rest (primary), red lines refer to the ones bound to the secondary BH. Solid and dot-dashed lines refer to WB, and SB particles.

the binary reaches separations where gravitational wave driven inspiral starts.

## ACKNOWLEDGMENTS

M.C. acknowledges MIUR under PRIN05 for financial support. S.K. acknowledges support by the U.S. Department of Energy through a KIPAC Fellowship at Stanford University and the Stanford Linear Accelerator Center.

## REFERENCES

1. J.W. Wadsley, J. Stadel, Th. Quinn, *New Astronomy*, Vol. 9, pp.137-158, 2004
2. J. Magorrian, S. Tremaine, D. Richstone, R. Bender, G. Bower, A. Dressler, S.M. Faber, K. Gebhardt, R. Green, C. Grillmair, J. Kormendy, T. Lauer, *The Astronomical Journal*, Vol. 115, pp. 2285-2305, 1998

3. S. Kazantzidis, L. Mayer, M. Colpi, P. Madau, V.P. Debattista, J.W. Wadsley, J. Stadel, Th. Quinn, B. Moore, *The Astrophysical Journal*, Vol. 623, pp. L67-L70, 2005
4. L. Mayer, S. Kazantzidis, P. Madau, M. Colpi, Th. Quinn, J.W. Wadsley, Proceedings of the Conference *Relativistic Astrophysics and Cosmology - Einstein's Legacy*, astro-ph/0602029
5. L. Hernquist, J.C. Mihos, *The Astrophysical Journal*, Vol. 448, pp. 41-63, 1995
6. L. Mayer, S. Kazantzidis, P. Madau, M. Colpi, Th. Quinn, J.W. Wadsley, Proceedings of the Conference, to appear in *Science*, 7 June 2007
7. R. Downes, P.M. Solomon, *The Astrophysical Journal*, Vol. 507, pp.615-654, 1998
8. V. Springel, T. Di Matteo, L. Hernquist, *MNRAS*, Vol. 361, pp. 776-794, 2005
9. J. Sèrsic, *Atlas de Galaxies Australes*, Observatorio Astronomico Cordoba, Argentina, 1968
10. J. Silk, M.J. Rees, *A&A*, Vol. 331, pp. L1-L4, 1998
11. A. King, *ApJ*, Vol. 596, pp. L27-L30, 2003
12. G.L. Granato, G. De Zotti, L. Silva, A. Bressan, L. Danese, *ApJ*, Vol. 600, pp. 580-594, 2004
13. V. Springel, N. Yoshida, S.D.M. White, *New Astronomy*, Vol. 6, pp.79-117, 2001
14. M. Dotti, M. Colpi, F. Haardt, *MNRAS*, Vol. 367, pp. 103-112, 2006
15. M. Dotti, M. Colpi, F. Haardt, L. Mayer, to appear in *MNRAS*, astro-ph/0612505, 2007
16. E.C. Ostriker, *The Astrophysical Journal*, Vol. 513, pp.252-258, 1999
17. S. Tremaine, et al. *The Astrophysical Journal*, Vol. 574, pp. 740-753, 2002